

Gas exchange with the ceramic superconductor $\text{YBa}_2\text{Cu}_3\text{O}_{7-\delta}$ and its fractal properties derived from results of small-angle neutron scattering

A. I. Okorokov, V. V. Runov, A. D. Tret'yakov, S. V. Maleev, and B. P. Toperverg

B. P. Konstantinov Leningrad Institute of Nuclear Physics, Academy of Sciences of the USSR, Gatchina

(Submitted 25 December 1990)

Zh. Eksp. Teor. Fiz. **100**, 257–273 (July 1991)

The irregular structure of specimens of the ceramic $\text{YBa}_2\text{Cu}_3\text{O}_{7-\delta}$ with densities $\rho = 3.5$ and 5.15 g/cm^3 has been studied by small-angle neutron scattering. It was found that the scattering intensity decreases strongly at temperatures below the boiling point of the gases O_2 , N_2 , and air surrounding the specimen. This phenomenon is due to condensation of the gas in the pores of the ceramic below the boiling point. It is concluded that the pore system is connected with the specimen's surface, which explains the ease of exchange between the ceramic and the surrounding medium (oxygen) on annealing. The dependence of the scattering intensity on the neutron momentum transferred is described by the law $I \propto q^{-n}$, where $n = 3.85 \pm 0.1$. Such a dependence, together with results on the absolute scattering intensity, is explained by the pore boundaries being very jagged and apparently having a more complicated structure than the usual surface fractal.

1. INTRODUCTION

After the discovery of high-temperature superconductivity a vast number of articles was published devoted to the superconducting properties of the new superconductors and of the compounds which were their "parents." Two facts were thus established which will be extensively used in what follows.

1. On relatively gentle heating, the superconducting ceramic compounds $\text{YBa}_2\text{Cu}_3\text{O}_{7-\delta}$ and $\text{La}_{2-x}\text{Sr}_x\text{CuO}_4$ exchange oxygen with the surrounding medium, and this strongly affects their superconducting properties. At the same time this exchange is suppressed for single crystals, and the higher the crystal quality the weaker the exchange (see, for example, Refs. 1–3).

2. Very weak magnetic fields ($H \ll 1 \text{ Oe}$) penetrate into ceramic superconductors. The lower critical field H_{c1} (the intragranule field) is of the order of hundreds of Oersted.⁴ This is explained by weak Josephson interaction of the ceramic grains with one another.⁵ Very intense theoretical and experimental studies of this behavior is going on at present (see, for example, Ref. 6 and the work quoted in it).

Both these phenomena—the oxygen exchange between the ceramic and medium and the low-field electrodynamic—are connected in an obvious way with the distribution of superconducting material in the ceramic and in particular with the voids (pores) present in the ceramic. It is, therefore, essential to study the static properties of these voids and also the extent of their connection with the medium surrounding the specimen. The present article is devoted to this. It should be remarked here that the study of the most varied porous media by various methods has recently developed greatly, in particular by using low-angle scattering of neutrons and of x-ray beams.^{7–12} Superconducting ceramics are a new class of porous materials with very unusual properties. It appears that the present work is the first study of them. It is usual to employ the concept of fractals to describe the porous structure of matter, which has been widely developed following the work of Mandelbrot (see, for example, Ref. 13). In discussing experimental results below we also use fractal language. Our main results are the following.

1. Most of the volume of voids in superconducting ce-

ramics consists of pores with dimensions on the order of 1000 \AA and more. Their surface is very jagged and is evidently a surface fractal.

2. The pores are well connected with the specimen surface, which is the reason for the very fast establishment of equilibrium between the gaseous content of the pores and the gas surrounding the specimen. In other words, the whole volume of the specimen is penetrated by a system of interconnected pores, which provides the transfer of gases (in particular of oxygen) from the external medium to practically all the ceramic grains.

3. Judging by the processes of liquefaction of gases in the pores, oxygen penetrates considerably more easily than nitrogen to the interior of the ceramic. In particular, if the specimen is surrounded by air, oxygen appears preferentially in the pores. Due to filling of the pores with oxygen, "oxygenation" and "deoxygenation" on heating occur by diffusion of oxygen over small distances on the order of the dimensions of the ceramic grains. This explains the easy exchange of oxygen between ceramic and surrounding medium and the difficulty of introducing oxygen into a single crystal. Experiments on changing the oxygen concentration over wide limits in a large single-crystal have only been reported in isolated papers (for example, Ref. 14). It appears that this crystal was, nevertheless, far from perfect. In this connection it seems to us essential to continue the investigations described below also for single-crystal systems of a different degree of perfection. Preliminary results of this work have been published.^{15,16}

2. INTERACTION OF GAS AND CERAMIC

Measurements of the angular dependence of the intensity of neutron scattering were made in the temperature range $4.2 \leq T \leq 300 \text{ K}$ and momentum transfer on scattering $0 \leq q \leq 2.6 \times 10^{-2} \text{ \AA}^{-1}$ ($\Delta q = 3 \times 10^{-3} \text{ \AA}^{-1}$) with an apparatus described elsewhere.¹⁷ A neutron beam with mean wavelength $\lambda = 10 \text{ \AA}$ and $\Delta\lambda/\lambda = 30\%$ was used in the experiment.

Helium gas was used to maintain the temperature for measurements in a cryostat. Measurements were also made of the angular dependence of scattering intensity at room

temperature without a cryostat. The external magnetic field on the specimen was less than 0.7 Oe and was directed along the beam axis.

Measurements were carried out on specimens of superconduction $\text{YBa}_2\text{Cu}_3\text{O}_{7-\delta}$ ceramics of different density:

1. $\rho = 3.5 \text{ g/cm}^3$ (dimensions $10 \times 30 \text{ mm}^2$; thickness 3 and 7 mm);¹⁾

2. $\rho = 5.15 \text{ g/cm}^3$ (dimensions $8 \times 32 \times 1.15 \text{ mm}^3$).²⁾

The specimens were tested by electrical resistivity, magnetic susceptibility, phase composition, etc. The temperature of the superconducting transition for the "loose" specimen 1 was $T_c = 93, 90,$ and 84 K (at the 0.95, 0.5, and 0.05 resistance levels, respectively) and for the "dense" specimen 2, $T_c = 93, 90, 85 \text{ K}$. Specimens prepared from the same materials were used^{18,19} for measurements of the frequency dispersion of the magnetic susceptibility and for studying magnetic flux penetration processes using muon spin resonance.

Measurements of the scattering intensity $I(q, T)$ were carried out after various procedures for treating the specimens. In the first experiments described by Axelrod *et al.*,¹⁵ the specimens 1 were heated in air to $T \approx 50\text{--}70 \text{ }^\circ\text{C}$ for several hours to reduce the moisture. They were then placed in the specimen unit of a tubular-type cryostat (tube volume $V \approx 400 \text{ cm}^3$) filled with helium gas and were rapidly (in $t < 30 \text{ min}$) cooled to $T = 4.2 \text{ K}$. The specimens were kept at low temperature for about three hours until there was no further change in $I(q)$, after which the scattering intensity on heating the specimen was measured. Afterwards pumping out of the specimens (tube with specimen) and subsequent treatment with different gases started: a) helium, b) oxygen, c) nitrogen.

For the helium treatment the specimen was maintained beforehand at room temperature for several hours *in vacuo* (10^{-3} atm), and the tube with the specimen was then filled with helium gas. The measurements of scattering intensity were then carried out at a given temperature, which was attained both on cooling and on heating the specimen after cooling to 4.2 K.

Oxygen and nitrogen treatment was carried out in the following way. The evacuated tube with the specimen at $T = 300 \text{ K}$ was first filled with helium, the temperature was then lowered to $T = 125\text{--}130 \text{ K}$ and a flask with the appropriate gas (oxygen or nitrogen) was connected to the tube. After this the temperature was further lowered to 4.2 K over a period on the order of one hour.

Filling with oxygen (nitrogen) was carried out from the gas volume $V_{\text{gas}} \approx 2000 \text{ cm}^3$ at a pressure $p \gtrsim 1 \text{ atm}$, so that the liquid phase comprised a small part of the tube volume. The condensate then accumulated at the bottom of the tube, not touching the specimen. After filling, the body of the tube with the specimen was connected to the helium vapor removal system. If necessary, part of the gas mixture (oxygen, nitrogen and helium) could be collected in the gas bulb and used for a recondensation. Measurements of the scattering intensity $I(q, T)$ were carried out while the specimen was heated from $T = 4.2 \text{ K}$ to the given temperature. The heating rate varied from 1 K/h (slow heating) to 10 K/h (rapid heating). All the temperature measurements presented here were carried out in the slow temperature change regime for the reason discussed below. The temperature control system maintained the running temperature to better than 0.1 K while statistics were collected, which varied within the limits

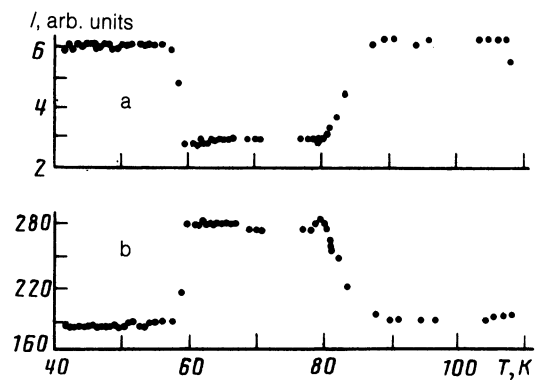


FIG. 1. Temperature dependence of neutron scattering intensity in the ceramic $\text{YBa}_2\text{Cu}_3\text{O}_{7-\delta}$ (specimen 1) for momentum transfer (a) $q = 7.8 \times 10^{-3} \text{ \AA}^{-1}$ and (b) $q \lesssim 3 \times 10^{-3} \text{ \AA}^{-1}$ (transmitted beam).

20–40 min for each temperature point. When a cooling-heating cycle of measurements was repeated part of the helium and oxygen (nitrogen) mixture which boiled off was partly let into the helium vapor removal system under a pressure $p \gtrsim 1 \text{ atm}$. On subsequent measurement cycles it was thus possible to reduce the oxygen (nitrogen) concentration in the specimen.

The results of measurements of the temperature dependence of the scattering intensity for $q = 7.8 \times 10^{-3} \text{ \AA}^{-1}$ and the intensity in the central detector, i.e., for $q \lesssim 3 \times 10^{-3} \text{ \AA}^{-1}$, are shown in Fig. 1. Results for specimen 1 with density $\rho = 3.5 \text{ g/cm}^3$ were obtained by the measuring procedure described above following Axelrod *et al.*,¹⁵ with measurements taken every 20 min.

As can be seen from Fig. 1, the scattering intensity is practically independent of temperature for $T > 90 \text{ K}$ and $T < 57 \text{ K}$ and is almost the same for these temperature regions. At the same time the scattering intensity falls sharply in the range $57 < T < 90 \text{ K}$ for all measured values of q , and simultaneously an increase in the transmitted beam ($q \lesssim 3 \times 10^{-3} \text{ \AA}^{-1}$) is observed. It is important to note that the transparency "window" and the magnitude of the effect depends on the cooling regime. In particular, the $I(q, T)$ dependence measured when the specimen is cooled and when it is heated come out differently. Also, on rapid heating, e.g., at a rate 10 K/h, a shift in the low-temperature boundary of the transparency window in the direction of high temperatures is observed.

Results were presented by Axelrod *et al.*¹⁵ where a hypothesis was also proposed to explain the observed effect. The main point of this hypothesis is that small-angle scattering occurs mainly at the voids of the ceramic which are partially filled with liquid oxygen in the temperature range $57 < T < 90 \text{ K}$. The difference in amplitude density, i.e., the contrast between matter and pore (see Table I) then decreases which, naturally, leads to a reduction in the scattering power of the medium. We note that this phenomenon can only be observed in the case when the relatively fine voids with dimensions on the order of 1000 \AA manage to get filled with condensate.

If the cooling occurs rapidly then condensation of gas directly into the solid phase in the form of a thin layer is possible, covering the walls of the ceramic pores more or less uniformly. On rapid cooling, the scattering at low temperature therefore remains at practically the same level as at tem-

TABLE I.

Chemical formula	Scattering amplitude b , 10^{-12} cm	density ρ , g/cm ³	No. of formula units per cm ³ , No. = 10^{20} cm ⁻³	Scattering amplitude density $N_0 b$, 10^{10} cm ⁻²	contract $[(N_0 b)_{123} - (N_0 b)]^2$, 10^{20} cm ⁻⁴
YBa ₂ Cu ₃ O ₇ (1-2-3- ceramic)	8,204	6,42	57,8	4,75	22,56 (air)
O ₂ (liq. $T = 90$ K)	1,161	1,14	21,4	2,49	5,11
O ₂ (sol. $T = 20$ K)	1,161	1,41	26,5	3,08	2,79
N ₂ (liq. , $T = 77$ K)	1,86	0,804	17,3	3,22	2,34
N ₂ (sol. $T = 20$ K)	1,86	1,03	22,1	4,12	0,4

peratures above the boiling point of the liquid filling the pores. If slow heating takes place after the cooling, then at temperatures above the melting point the liquid phase penetrates into the small pores due to the capillary effect and (or) fills the fine serrations on the surface of large pores. Confirmation of these ideas comes from the fact that, as follows from subsequent experiments carried out in an oxygen atmosphere in measurements in the slow cooling regime from room temperature, only the upper limit of the transparency window on the $I(q, T)$ curve is observed, while the low-temperature boundary, corresponding to the freezing point, hardly registers.

A number of questions arise in connection with the phenomena observed. First, what gas condenses in the pores and what is its source? Second, what is the structure of these pores and their surfaces? Finally, how does the porosity of superconducting ceramics affect their physical properties?

We note first that the boundaries of the transparency window coincide to a remarkable degree with the boiling point (90 K) and melting point (54 K) of oxygen. As a consequence of this the suggestion was made¹⁵ that it was oxygen which condensed in the pores. We give here the results of experiments confirming this suggestion and answering the question of the source of oxygen in the pores.

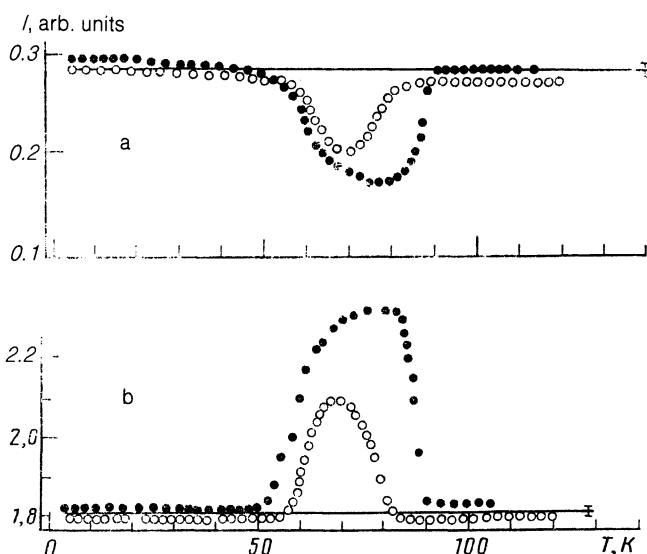


FIG. 2. Temperature dependence of intensity of neutron scattering by specimen 1: a) for momentum transfer $q = 5 \times 10^{-3} \text{ \AA}^{-1}$; b) intensity of transmitted beam ($q < 3 \times 10^{-3} \text{ \AA}^{-1}$). Solid line—scattering by specimen in vacuo at $T = 300$ K and helium filled; full circles are scattering by the specimen filled with oxygen, open circles are with nitrogen.

The temperature dependence of the scattering intensity for $q = 5 \times 10^{-3} \text{ \AA}^{-1}$ and of the neutron beam intensity for $q < 3 \times 10^{-3} \text{ \AA}^{-1}$ is shown in Fig. 2 for a ceramic with density $\rho = 3.5 \text{ g/cm}^3$ for different gas treatment, described in the previous section. The results of similar experiments for a ceramic with density 5.15 g/cm^3 are given in Fig. 3.

It can be seen from Figs. 2 and 3 that for filling the ceramic pores with helium the scattering intensity is independent of temperature over the whole measuring interval. Moreover, it does not depend on the cooling regime and stays constant for cyclic temperature changes. It follows from these observations that the procedure for removing condensed gas from the ceramic described above is completely effective. This shows that the pore system in which the gas is condensed is open, i.e., is connected with the surface of the specimen and its source is the external medium.

Also, in these figures results are given obtained from treatment of the specimens with oxygen ($T_b = 90.17$ K, $T_m = 54$ K at normal pressure) and nitrogen ($T_b = 77.4$ K, $T_m = 63.3$ K). It is seen from Figs. 2 and 3 that, indeed, the features on the curves of the temperature dependence are close to the temperatures of melting and boiling of the gases used in the treatment of the ceramic. The low-temperature discontinuity is only sharply marked when the pores are filled with a relatively small amount of gas, while the high-temperature one is always clearly distinguished. When the pores are filled with a large quantity of gas the scattering intensity at low temperatures is appreciably lower than in the high temperature region. This is evidence of the partial filling of scattering voids with solidified gas at temperatures below its freezing temperature. Such filling can, of course,

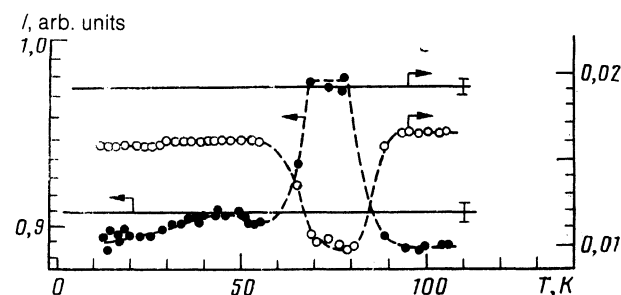


FIG. 3. Temperature dependence of intensity of neutron scattering by specimen 2 for $q = 5 \times 10^{-3} \text{ \AA}^{-1}$ (right hand scale) and the transmitted beam $q < 3 \times 10^{-3} \text{ \AA}^{-1}$ (left hand scale). The full upper and lower straight lines correspond to intensities of scattering and of the transmitted beam for the specimen in vacuo at $T = 300$ K and filled with helium. The closed and open circles correspond to the intensities of scattering and of the transmitted beam for the specimen filled with oxygen.

occur if the amount of this gas is sufficiently great so that part of it does not manage to transform to the solid phase during cooling and penetrates to the pores in the liquid state, where it freezes. Reduction in the filling of the pores with gas was achieved by heating the specimen above the boiling point with subsequent cooling and repetition of the heating cycle, as described above. As a result, the discontinuity on the scattering curve at $T = T_m$ appeared more sharply, while the scattering intensity in the region $T < T_m$ increased. Also, when the number of cycles of such treatment was not too large the intensity $I(q, T)$ for $T_m < T < T_b$ stayed at the same level and started to decrease on further cycling.

It should be remarked that it is rather difficult (see below) to make a reliable quantitative estimate of the gas condensed in the specimen. However, one important conclusion can be drawn from the experimental results. It follows from a comparison of Figs. 1–3 that the boundary of the transmission window for a specimen in preliminary contact with air (Fig. 1) coincides with the discontinuities on the $I(q, T)$ dependence when the specimens were treated in an oxygen atmosphere (Figs. 2, 3). It can therefore be suggested that 1-2-3 ceramics are sorbents of oxygen which mainly fill the fine pores.

That nitrogen is adsorbed less well by the superconducting ceramic is also confirmed by the weaker than expected "illumination" effect, on the basis of the corresponding contrast (see Table I) on treating the specimen in nitrogen, compared with oxygen. This effect is, in general, not unexpected. It can, however, be very important in studying processes of oxygen penetration into the structure of high- T SC's, because when the surface of a ceramic pore is strongly developed (see below), even at temperatures above the oxygen boiling point a fairly large amount of it can be contained in them in the form of a thin surface layer.

3. TEMPERATURE DEPENDENCE OF THE RESISTANCE

The oxygen boiling point is close to the superconducting transition temperature for 1-2-3 ceramics, at least for specimens prepared in our experiments. This coincidence is most likely fortuitous. Nevertheless, to elucidate its role and also the conditions of oxygen boiling in the pores special experiments were carried out on the change in the resistance of specimens when they were treated in different gaseous media: helium, nitrogen, and oxygen.

The experimental arrangement for measuring the resistance of ceramic specimens is shown in Fig. 4b. The specimen was housed in a thermostated specimen tube with helium as exchange gas. A semiconductor resistance thermometer was firmly attached to the specimen. The specimen resistance $R(T)$ was measured by a four-probe system. Where $R(T)$ changed sharply the mean temperature over the volume of the specimen could be judged from the specimen resistance, while the semiconductor thermometer indicates the temperature near the surface. The experiment was carried out in various heating-rate regimes: 0.1–0.01 deg/min. Experimental results for a heating rate of 0.1 deg./min are shown in Fig. 4a. The lower part of the $R(T)$ curve is the same for all gases. The resistance at high temperatures ($T > 95$ K) differs slightly; this could be associated with residual effects after boiling off the liquid. In the case of oxygen a constant resistance R is observed in the temperature region 90–95 K, which we associate with the delay of the

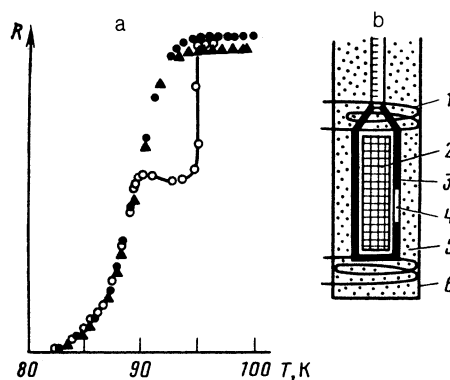


FIG. 4. Temperature dependence of the resistance $R(T)$ when specimen 1 is immersed in various media: (\blacktriangle) helium, (\bullet) nitrogen and (\circ) oxygen; a) experimental results; b) measuring arrangement: 1) spiral heater, 2) specimen, 3) holder frame, 4) thermometer, 5) exchange gas, 6) temperature-controlled tube.

specimen temperature while the oxygen boils off from its pores. The delay takes place at the temperature $T = 90$ K corresponding to the boiling point of oxygen under normal conditions.

Measurements were also made in an oxygen environment at elevated oxygen pressure. In the experiment the inside of the specimen tube was connected to an oxygen cylinder at pressures 4 and 10 atm. The volume of the cylinder was such that when oxygen condensed in the tube the pressure in the system decreased by less than 10%. Measurements of the $R(T)$ curves under these conditions did not reveal a noticeable shift towards high temperatures compared with Fig. 4. There is also no anomaly at $T = 90$ K. It is known from handbook data that at pressures of 4 and 12 atm the boiling point of oxygen is 105 and 122 K. It is not possible to notice an anomaly in R in this temperature region by our method, since the resistance here is weakly dependent on temperature. However, the absence of a shift in $R(T)$ as the oxygen pressure rises points to the lack of a connection between T_c and T_b for oxygen, as would be expected. It should be mentioned that the oxygen anomaly in Fig. 4a may be the reason for the distortion in the shape of $R(T)$ sometimes observed in experiments on high- T SC's.

4. ANGULAR DISTRIBUTION OF SCATTERED NEUTRONS

It can be concluded from all the previous discussion that a ceramic superconductor has a branched system of pores connected with the surface of the specimen. We will call such a system of pores open. Oxygen is adsorbed in such a system. The question naturally arises about the structure and statistical characteristics of this porous medium. A careful analysis was carried out of the dependence of the scattering intensity on transferred neutron momentum q to study this question. Since small-angle scattering was very intense, single-scattering-regime experiments were then carried out on specimens of various thicknesses for control purposes. Several specimens with transverse dimensions of 15×8 mm² and thicknesses 0.67 ± 0.01 and 1 ± 0.02 mm (2 samples) were prepared from a single piece of 1-2-3 ceramic of density 5.15 g/cm³. From them specimens were formed of five thicknesses: 0.67, 1.66, 2.33, 3.32 and 3.9 mm. This set was used both to determine the absorption and the total neutron scattering. In the first case the specimens were placed directly in

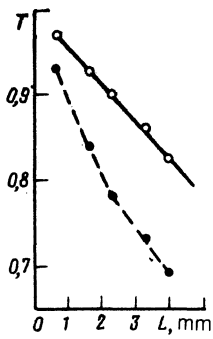


FIG. 5. Dependence of transmitted neutrons on the thickness of specimen L , related to (○) neutron attenuation and (●) integral scattering.

front of the detector so that all the neutrons falling in the solid angle $\Delta\Omega \approx 2\pi$ should fall on it. The dependence of the neutron absorptive transmission coefficient $T_a = I_a/I_0$ on the specimen thickness L , where I_a is the neutron beam intensity incident on the detector and I_0 is the intensity of the incident beam, is shown in Fig. 5. The dependence on L of the integral scattering intensity T_s is also shown there, determined from the reduction in neutron intensity incident on the central counter under normal geometry.

It can be seen from this figure that the dependence on L of both $T_a(L)$ and $T_s(L)$ is close to linear, and as it should, the extrapolation to $L = 0$ gives $T_a(0) = T_s(0) = 1$. Therefore, at least for the first three or four values of the thickness L the effects of multiple scattering can be neglected. This conclusion is also confirmed by the linear dependence of the neutron scattering intensity $I(q)$ on L . The single scattering for the momentum transfer region achieved in our experiments ($q \geq 3 \times 10^{-3} \text{ \AA}^{-1}$) guarantees the applicability of the Born approximation for describing the scattering. In actual fact, as it is easy to convince oneself by simple estimates, the characteristic momentum transfers on refraction at the ceramic voids should be less than or of order 10^{-4} \AA^{-1} (see the following section). But then in our experiments it was only possible to observe diffraction for multiple scattering. However, in that case the linear law of thickness dependence of scattering intensity would break down.

Having thus convinced ourselves that the scattering is a weak effect, we write the following expression for the neutron intensity $I(\Omega)$ incident on the detector at an angle Ω :

$$I(\Omega) = I_0 \Phi(\Omega) \left\{ 1 - \left[\frac{1}{l_a} + \int \frac{d\Omega'}{l(\Omega')} \right] L \right\} + I_0 \int \frac{d\Omega' \Phi(\Omega') L}{l(\Omega - \Omega')} + I_b(\Omega) + I_b^h, \quad (1)$$

where I_0 is the neutron beam intensity incident on the specimen, $\Phi(\Omega)$ is its shape function normalized to unity,

$$\int d\Omega \Phi(\Omega) = 1, \quad (2)$$

l_a is the mean free path determined by the attenuation, L is the specimen thickness, $I_b(\Omega)$ is the neutron scattering intensity at the casing of the apparatus, and I_b^h is the room background. In conformity with the general theory of scattering by a nonuniform medium (see, for example, Teixeira⁷). The value of $l^{-1}(\Omega)$ is determined by the relation

$$l^{-1}(\Omega) = [\delta(bN_0)]^2 \int d\mathbf{r} e^{i\mathbf{r} \cdot \mathbf{q}} \langle \rho(\mathbf{r}) \rho(0) \rangle = N_0^{-1} \frac{d\sigma}{d\Omega}, \quad (3)$$

where b is the amplitude of the scattering by one formula unit of $\text{YBa}_2\text{Cu}_3\text{O}_7$, N_0 is the number of these units in unit volume, $N_0 b$ is the amplitude density of scattering, $[\delta(bN_0)]^2$ is the contrast in scattering amplitude (see Table I), $\rho(\mathbf{r}) = 1$ if the point \mathbf{r} is in the medium and $\rho(\mathbf{r}) = 0$ for \mathbf{r} in a pore; the angular brackets indicate spatial averaging and $d\sigma/d\Omega$ is the mean scattering cross-section of a pore.

A careful consideration of the different contributions to the observed scattering is essential since first, the scattering intensity in our case falls fairly rapidly with an increase in scattering angle and for large angles the terms in Eq. (1) which depend weakly on Ω start to play an appreciable role and secondly, a noticeable distortion of $I(\Omega)$ arises for limitingly small angles if the shape of the incident beam $\Phi(\Omega)$ is not taken into account properly.

There are terms in Eq. (1) proportional to the specimen thickness L and terms independent of it, i.e.,

$$I(\Omega) = I_0 A(\Omega) L + B. \quad (4)$$

Analysis of the experimental results for four independent measurements with different thicknesses L showed that the value of A to within 5% is really independent of L for all scattering angles. In other words, it is not necessary to invoke a more complicated dependence on L (for example, L^2) to this accuracy, i.e., the scattering can be considered single.

Our apparatus¹⁷ contains 20 scattered-neutron detectors. Averaging Eq. (4) over the angular dimensions of each detector δ_k , where k is the detector number, we find for the observed value of A_k , taking account of Eq. (1)

$$A_k = \int d\Omega \Phi_k(\Omega) l^{-1}(\Omega) - (l_a^{-1} + l_s^{-1}) \Phi_k(0), \quad (5)$$

$$\Phi_k(\Omega) = \int_{\delta_k} d\Omega_1 \Phi(\Omega - \Omega_1),$$

where $l_s^{-1} = \int d\Omega l^{-1}(\Omega)$ is the scattering free path.

We have expressed the scattering law, as is generally done,⁷⁻¹³ in the form

$$l^{-1}(q) = S_0 q^{-n}, \quad (6)$$

where $q^2 = k^2(\theta_x^2 + \theta_y^2)$ is the momentum transfer, $k = 2\pi/\lambda$, λ is the neutron wavelength averaged over the spectrum, and θ_x and θ_y are the horizontal and vertical components of the scattering solid angle Ω , respectively. Such a power-law dependence can arise in the case of a wide distribution of scatterers in the range of dimensions $R_{\max} \gg R_{\min}$, if the conditions

$$R_{\max}^{-1} \ll q \ll R_{\min}^{-1} \quad (7)$$

are satisfied.

The constant S_0 in Eq. (6) depends on the scattering amplitude contrast and the maximum dimensions of the scattering inhomogeneities R_{\max} . The index n is associated with the anomalous (fractal) dimensionality of the pore surface (see below). The value of l_a^{-1} is known from independent measurements, while l_s^{-1} can be determined by integrating $l^{-1}(q)$ over all scattering angles.³⁾

In Eq. (5) from A_k the quantity $l_a^{-1} + l_s^{-1}$ occurs. It is easy to find this by measuring the neutron intensity incident on the central detector. The value of A_0 determines this intensity. If the scattering into the central counter is small

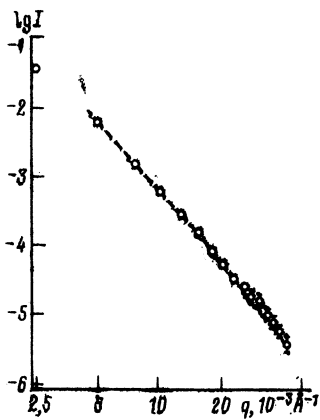


FIG. 6. Experimental results for $I(q)$ (points) and calculated curve $I(q) \propto q^{-n}$ with $n = 3.85$, convolved with the instrumental resolution function (dashed line).

compared with the weakening of the transmitted beam associated with scattering into other detectors and the attenuation, then in fact

$$A_0 = -\Phi_0(l_0^{-1} + l_s^{-1})$$

holds. As a result, we obtain for the value of A_k

$$A_k = \int_{\delta_k} d\Omega \Phi_k(\Omega) l^{-1}(\Omega) + A_0 \Phi_0^{-1}. \quad (8)$$

This formula was used to analyze the experimental results.

The resolution function of the apparatus was approximated by a Gaussian with dispersion $\sigma = 2.7 \times 10^{-3} \text{ \AA}^{-1}$, which was determined by the slit geometry. Only the vertical divergence of the beam was taken into account for this since the horizontal was almost an order of magnitude smaller.

The experimental results and the theoretical curve with the scattering law of Eq. (6) with $n = 3.85$ are shown in Fig. 6 on a double logarithmic scale, convolved with the apparatus resolution function. It follows from Eq. (6) that in fact the function $l^{-1}(q)$ decreases with increasing q according to a power law with exponent $n = 3.85 \pm 0.1$, and the departure from this law in the small momentum region is not noticeable, which is evidence of the sufficiently large values of R_{\max} . In actual fact, an attempt to determine the value of R_{\max} with the help of the model formula

$$l^{-1}(q) = S_0 (\kappa^2 + q^2)^{-n/2}, \quad (9)$$

where the three parameters S_0 , $\kappa = R_{\max}^{-1}$ and n were varied, gave the following results: $\kappa = (0.07 \pm 0.55) \times 2.5 \times 10^{-3} \text{ \AA}^{-1}$, $n = 3.82 \pm 0.1$ and the quality criterion for the fit was not improved compared with Eq. (6). It can thus be considered with some certainty that if a wide distribution of scattering inhomogeneities exists over sizes in the range between R_{\min} and R_{\max} , then in the momentum transfer interval obtaining in our experiment the inequality of Eq. (7) holds.

In the following section we will consider in detail the question of the nature of the inhomogeneities. It should only be remarked here that the filling of these irregularities by condensed gas does not noticeably change the scattering law, although we did not carry out a detailed study in these cases. It is also not possible without additional hypotheses or ex-

periments (for example, on weighing) to determine the amount of adsorbed liquids.

5. DISCUSSION OF RESULTS

One of the main results obtained is the power of the angular dependence of neutron scattering by the pore system in the ceramic: $l^{-1}(q) \propto q^{-n}$, where the exponent n is close to four, i.e., to the value characteristic for scattering by finite sized irregularities (the Porod law). The scattering power law indicates that the pores which contribute to the scattering are sufficiently large so that the condition $q_{\min} R_{\min} \gg 1$ is satisfied. A more exact practical criterion for the characteristic minimum size was proposed by Bale and Schmidt:⁸ $q_{\min} R_{\min} \approx 3.5$. We will use it in what follows. In our experiments we took $q_{\min} = 3 \times 10^{-3} \text{ \AA}^{-1}$ and we obtain for the minimum $R_{\min} \approx 1.2 \times 10^3 \text{ \AA}$. We now try to elucidate whether our results actually correspond to scattering by such irregularities with characteristic dimension $R_{\min} = R$. For simplicity in the calculations we will consider these irregularities to be spheres. As is well known, for $qR \gg 1$ the scattering cross-section has the form

$$\frac{d\sigma}{d\Omega} = (N_0 b)^2 \frac{8\pi^2 R^2}{q^4}. \quad (10)$$

If all the pores in a specimen have radius R , then the density of pores c is determined by the obvious relation

$$\frac{\Delta\rho}{\rho} = \frac{4\pi R^3 c}{3}, \quad (11)$$

where $\Delta\rho = \rho_0 - \rho$ is the difference in density between the specimen and the maximum possible value ρ_0 . By using these expressions for the relative scattering intensity in the solid angle interval $\Delta\Omega$ we find

$$\frac{\Delta I}{I_0} = \frac{\Delta\rho}{\rho} (N_0 b)^2 \frac{6\pi L \Delta\Omega}{R q^4} = \frac{L \Delta\Omega}{l(q)}. \quad (12)$$

If we now use our values for $\Delta I / I_0$ and take account of the resolution of the apparatus, then we obtain $R \approx 1900 \text{ \AA}$ for a specimen with $\rho = 5.15 \text{ g/cm}^3$ from Eq. (2). This value of R is close to the minimum estimate obtained above, $R_{\min} \approx 1200 \text{ \AA}$. Our estimate was made using the "maximum," i.e., on the assumption that all pores contribute to the observed scattering. It is possible that some of the pores are very small and do not contribute to the observed angular distribution while some are so large that scattering by them occurs in the refraction regime at very small angle and does not contribute to the observed scattering intensity. In both cases the effective number of pores contributing to the observed scattering will be less than the number determined by Eq. (11) and, correspondingly, requires a smaller value of R for the observed scattering intensity. In this way the experimental results obtained cannot be explained, starting from the suggestion about the scattering by a system of pores with characteristic size R .

Before proceeding further, we show that refraction by large pores cannot contribute to the observed scattering. We note that the matter-vacuum refractive index n_0 for this is obtained from the relation $1 - n_0 = N_0 b \lambda^2 / 2\pi$. The quantity on the right-hand side is of the order of the angle of refraction θ_r . As a result, using data in tables for $\text{YBa}_2\text{Cu}_3\text{O}_7$, we obtain

$$\theta_r \approx 8 \cdot 10^{-5} \text{ rad}, R_r = \lambda / \theta_r \approx 1,2 \cdot 10^5 \text{ \AA}, \quad (13)$$

where R_r is the minimum possible size of the region at which refraction takes place. For $R < R_r$, the scattering proceeds in the refractive regime and is described by the usual Born expression used above.

The region of momentum transfers corresponding to refraction is determined by the condition

$$q < q_r = \frac{2\pi}{\lambda} \theta_r = 5 \cdot 10^{-5} \text{ \AA}^{-1}.$$

This value is appreciably less than the angular width of a separate detector Δq in our apparatus ($\Delta q = 3 \times 10^{-3} \text{ \AA}^{-1}$). Even in the case of multiple refraction all the refracted neutrons should be scattered within the limits of the first detector. In fact, the following upper estimate for the least-square deviation of refracted neutrons is valid:

$$(\overline{q^2})^{1/2} \leq q_r (L/R_r)^{1/2} \approx 5 \cdot 10^{-4} \text{ \AA}^{-1}. \quad (14)$$

We assumed here that the whole ceramic is penetrated by voids of the order of R_r , and the number of voids is a maximum. This is evidently very much an overestimate.

We now consider to what effect we can ascribe the deviation from the fourth power of n in the dependence in Eq. (6) of the scattering intensity on q . According to the experimental results, the exponent is somewhat less than 4 and is equal to 3.85 ± 0.1 . As is well known, an exponent $n < 4$ corresponds to scattering by irregularities of the fractal type, which are characterized by a broad size distribution. If, then, $n < 3$ holds, the scattering objects are normal volume fractals, but for $3 < n < 4$ two possibilities exist. First, the object may consist of pores with a strong surface development, so that if the total area of the surface of a pore measured on the scale of the pore dimension R is proportional to R^2 , then on measuring the surface on a scale $r \ll R$ the area of the surface is of the order of $R^2 (R/r)^\Delta$, where $0 < \Delta < 1$ and $n = 4 - \Delta$. The fractal dimensionality of the surface, $D = 2 + \Delta$, is greater than two. This case has been discussed by Tu *et al.*,¹ Couach *et al.*² and by Teixeira.⁷ Another possibility was considered by Wong,¹⁰ who proposed a model in which pores of dimension R are distributed according to the rule

$$dN/dR = A (R_{\max}/R)^{3+\Delta}. \quad (15)$$

We start with an analysis of the first possibility, a surface fractal. Since we are interested in the absolute value of the cross section, we must determine more accurately than is usually done⁷⁻¹² the exponent which enters the expression for the cross section. It is, evidently, most convenient to use the argument of Bale and Schmidt.⁸ There the scattering intensity was expressed in terms of the constant N and the dimensionality of the surface fractal $D = 2 + \Delta$. These quantities are determined by the relation

$$n_r = N r^{-D}, \quad (16)$$

where n_r is the number of blocks of size r covering the fractal surface when the dimension r is small compared with the dimensions of a pore R . In addition, it is evident from considerations of matching that for $r \sim R$ the number n_R is of the order of unity, from which we find $N \propto R^\Delta$. As a result, using the equations of Bale and Schmidt,⁸ we obtain instead of Eq. (12)

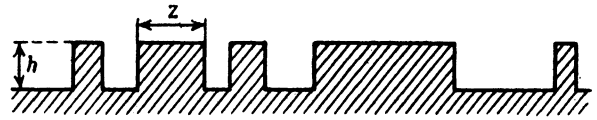


FIG. 7. A surface covered with asperities of height h with a wide distribution of transverse dimensions z .

$$\frac{\Delta I}{I_0} = \frac{\Delta \rho}{\rho_0} (N_0 b)^2 \frac{6\pi\alpha L}{Rq^4} (Rq)^\Delta \Delta \Omega, \quad (17)$$

where R is some effective pore size and α is a numerical factor of order unity which cannot be obtained theoretically without some detailed model of the fractal surface being specified. This expression differs from Eq. (12) parametrically by the large factor $(qR)^\Delta$. In our case we have $\Delta \approx 0.15$, i.e., it is small and really of the order of unity. So, for $q = 1.5 \times 10^{-2} \text{ \AA}^{-1}$ and $R = 10^4 \text{ \AA}$, we have $(qR)^{0.15} = 2.1$. Thus, taking account of this factor somewhat increases the scattering intensity and at the same time allows an increase in the minimum estimate for R . However, as was noted at the end of Sec. 4, no departure from the power behavior of $I(q)$ was observed and consequently $q_{\min} R_{\min}$ really is large. Even considering the fractal nature, the lower estimate for R thus appears insufficiently large. This is, of course, valid if all dimensionless constants, for example α in Eq. (17), are of order unity. What has been discussed can be considered an indication that the surfaces of the pores have a more complex structure than an ordinary surface fractal. It is apparent that the existing experimental results are insufficient for determining this structure. We therefore consider one simple model which allows us to explain the experimental results. The essence of this model is the following. The surface of the pores is covered with asperities, with height h and transverse dimension z , and there is a wide distribution of these transverse dimensions from a minimum value $z_0 \ll h$ to a maximum value $z \sim R$ (see Fig. 7). We determine the size distribution law for the asperities in the following way. The maximum number of asperities of size z on the surface of a pore of radius R can, evidently, be written as:

$$N_m(z) = 4\pi A (R/z)^2,$$

where $A \sim 1$. We assume that the size distribution law for asperities is of the form

$$\frac{dN}{dz} = N_m(z) \frac{1}{z_0} \left(\frac{z_0}{z}\right)^\Delta e^{-\kappa z} = 4\pi A \left(\frac{R}{z_0}\right)^2 \left(\frac{z_0}{z}\right)^{2+\Delta} \frac{e^{-\kappa z}}{z_0}, \quad (18)$$

where $\kappa \sim R^{-1}$. It is shown in the Appendix that in the case considered for $\Delta I/I_0$ when $qR \gg 1$ the following expression holds

$$\frac{\Delta I}{I_0} = \frac{\Delta \rho}{\rho} (N_0 b)^2 \frac{6\pi\alpha_1 L}{Rq^4} \left(\frac{h}{z_0}\right) (qz_0)^\Delta \Delta \Omega, \quad (19)$$

where $\alpha_1 \sim 1$. If the ratio h/z_0 is sufficiently large, then $\Delta I/I_0$ can have the necessary value, even though $qz_0 < 1$ holds, since for $\Delta \ll 1$ we have $(qz_0)^\Delta \sim 1$.

We now return to the model of spherical pores distributed according to the law of Eq. (15) (Ref. 10). In this case we obtain for $qR_{\max} \gg 1$

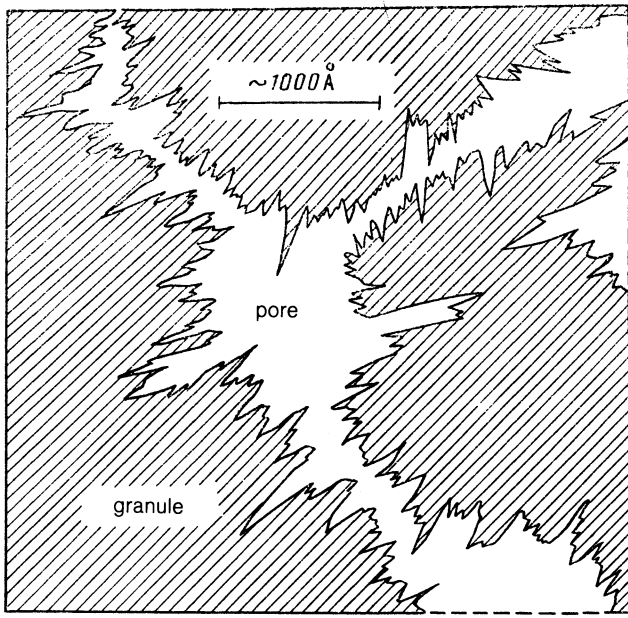


FIG. 8. The picture of irregularity in a ceramic derived from results of small-angle neutron scattering.

$$\frac{\Delta I}{I_0} = \frac{\Delta \rho}{\rho} (N_0 b)^2 \frac{4\pi}{3} (1-\Delta) \frac{(qR_{max})^\Delta}{q^\Delta R_{max}} c_\Delta, \quad (20)$$

$$c_\Delta = \int_0^\infty \frac{dx}{x^{1+\Delta}} \left(\cos x - \frac{\sin x}{x} \right)^2.$$

For $\Delta = 0.01, 0.2$ and 0.3 we obtain correspondingly for c_Δ the values 2.6, 2.0 and 1.5. Such a small value of c_Δ does not allow us to obtain a large value for the scattering at high q . The model proposed by Wong¹⁰ is thus unable to explain the experimental results.

6. CONCLUSIONS

Our main result can thus be summarized in three statements. First the pore system in the ceramic $\text{YBa}_2\text{Cu}_3\text{O}_{7-\delta}$ is closely connected with the surface of the specimen, i.e., it is open. The surrounding gas therefore penetrates easily inside the ceramic.

Second, the bulk of the ceramic pores have characteristic dimensions R at least of the order of several thousand Ångström, while the surface of the pores is extremely strongly developed (see Fig. 8) and evidently has a more complicated structure than an ordinary surface fractal. This structure is characterized by two parameters: the ratio of the depth of modulation of the surface irregularities h and their minimum width z_0 and the exponent Δ describing the power law of the distribution of longitudinal dimensions of the corrugations z .

Thanks to these two features the surface of the ceramic grains is well connected with the gaseous medium surrounding the specimen. On heating, a ceramic grain therefore easily exchanges oxygen with the external medium: in order to reach a certain point inside the specimen an oxygen atom only has to diffuse inside a grain from the surface of the nearest pore.

Third, the ceramic studied adsorbs oxygen more

strongly than nitrogen and preferentially collects oxygen from the surrounding atmosphere.

The authors thank B. Mandelbrot for valuable discussion of the results of this work, E. G. Ponyatovskii for supporting this work, N. M. Kotov, A. S. Nigmatullin, Ya. M. Mukovskii, V. K. Fedotov, R. K. Nikolaev and N. S. Sidorov for preparation and testing of the specimens, D. N. Aristov for numerical calculations, L. A. Aksel'rod, G. P. Gordeev, V. P. Grigor'ev, V. N. Zabenkin, I. M. Lazebnik, V. T. Lebedev, V. N. Slyusar', R. Z. Yagud, I. N. Ivanov, É. B. Rodzevich, N. M. Kusova and G. V. Stepanova for help in the work and its design.

The work is supported by the Scientific Council on the Problem of H-T SC's and is carried out within the framework of Project No. 2 "Shkala" of the Government Program "High-temperature superconductivity."

APPENDIX

The pore scattering cross-section can be expressed in the form²⁰

$$\frac{d\sigma}{d\Omega} = (bN_0)^2 \int_{V_p} d\mathbf{r}_1 d\mathbf{r}_2 \exp[iq(\mathbf{r}_1 - \mathbf{r}_2)], \quad (A1)$$

where the integration with respect to \mathbf{r}_1 and \mathbf{r}_2 is carried out over the pore volume. Introducing the vector $\xi = \mathbf{r}_1 - \mathbf{r}_2$ we obtain²⁰ from Eq. (A1)

$$\frac{d\sigma}{d\Omega} = (bN_0)^2 \int_{V_p} d\xi V(\xi) e^{iq\xi}, \quad (A2)$$

where $V(\xi)$ is the common volume of two identical pores shifted by the vector ξ . Evidently, we have for $\xi \rightarrow 0$ $V(\xi) = V_p - \xi V'$ where $V_p \approx 4\pi R^3/3$ is the pore volume and $V' > 0$. We find from Eqs. (A2) and (11)

$$\frac{\Delta I}{I_0} = \frac{\Delta \rho}{\rho} (N_0 b)^2 J(q) L \Delta \Omega, \quad (A3)$$

$$J(q) = \int d\xi \langle V(\xi) \rangle e^{iq\xi} = \frac{4\pi}{q} \int d\xi \xi \langle V(\xi) \rangle \sin q\xi, \quad (A4)$$

where the angular brackets indicate averaging over the whole shape of the pores of dimensions R . Integrating $J(q)$ by parts, we obtain

$$J(q) = -\frac{4\pi}{q^3} \int d\xi \sin q\xi \frac{d^2}{d\xi^2} [\xi \langle V(\xi) \rangle]. \quad (A5)$$

The asymptote of this expression for large q is evidently determined by the behavior of the integrand from small shifts ξ . The change in $\langle V(\xi) \rangle$ then occurs because of the relative shift of each of the projections of the surface [see the description of the model before Eq. (18) (Fig. 7)]. The volume of an asperity is of order $z^2 h$ and its change depends on the direction of the displacement. For each actual pore, then, due to its closure on displacement by the vector ξ , part of the asperities shift perpendicularly to the surface of the grains, and part parallel. However, small ξ are distinguished in the distribution function, Eq. (18), and thus only asperities displaced parallel to the surface are of interest. The reduction in the volume of an asperity is of order $zh\xi$, this expression being valid only for $\xi < z$, while for $z \ll \xi$, because of the irregularity of the pore surface, the corresponding contribution to $\langle V(\xi) \rangle$ decreases. Therefore

$$\langle V(\xi) \rangle = V_p - h z^2 f(\xi/z), \quad (\text{A6})$$

where $f(\infty) = 0$. Substituting Eq. (A6) into Eq. (A5) and taking account of Eq. (18), we find

$$\begin{aligned} J(q) &= \frac{4\pi A h R^2}{q^3} \int_{z_0}^{\infty} \frac{dz}{z_0} \left(\frac{z_0}{z}\right)^{2+\Delta} e^{-\kappa z} \int_0^{\infty} d\xi \sin q\xi \frac{d^2}{d\xi^2} \left[z^2 \xi f\left(\frac{\xi}{z}\right) \right] \\ &= \frac{4\pi A h R^2}{q^3} \int_0^{\infty} dx \frac{d^2}{dx^2} [x f(x)] \int_1^{\infty} \frac{dy}{y^\Delta} e^{-\kappa y} \sin(q z_0 x y), \end{aligned} \quad (\text{A7})$$

where $\kappa z_0 \ll q z_0 \ll 1$ and so in the integral over y the lower limit can be replaced by zero. We obtain as a result

$$\begin{aligned} J(q) &= \frac{4\pi A h R^2}{q^3} \Gamma(1-\Delta) \sin\left[\frac{\pi}{2}(1-\Delta)\right] \\ &\quad \times \frac{h}{z_0} (q z_0)^\Delta \int_0^{\infty} \frac{dx}{x^{1-\Delta}} \frac{d^2}{dx^2} [x f(x)], \end{aligned} \quad (\text{A8})$$

where, taking account of Eq. (A3), we obtain Eq. (18).

¹⁾ Prepared in the Institute of Steel and Alloys, Moscow.

²⁾ Prepared in the Institute of Solid State Physics, Chernogolovka.

³⁾ One should obviously, then, use the parameters S_0 and n obtained from the fit of the results to Eq. (5). On the other hand, it is clear that for $n \geq 2$ the integral of $l^{-1}(q)$ over q will diverge in the vicinity of $q = 0$ and it must be cut off at some characteristic minimum momentum $\kappa_{\min} = 1/R_{\max}$. Unfortunately it was not possible to carry out this program.

¹K. N. Tu, C. C. Tsuei, S. I. Park, and A. Levi, Phys. Rev. B **38**, 772 (1988).

²M. Couach, A. F. Khoder, F. Monnier, B. Barbara, and J. Y. Henry, Phys. Rev. B **38**, 748 (1988).

³K. N. Tu, N. C. Yeh, S. I. Park, and C. C. Tsuei, Phys. Rev. B **39**, 304 (1989).

⁴H. Maletta, A. P. Malozemoff, D. C. Cronmeyer, C. C. Tsuei, R. L. Greene, J. G. Bednorz, and K. A. Müller, Solid State Commun. **62**, 323 (1987).

⁵J. R. Clem, Physica (Utrecht) C **153-155**, 50 (1988).

⁶I. D. Luzyanin, S. L. Ginzburg, V. P. Khavrovin, and G. Yu. Logvinova, Phys. Lett. A **141**, 85 (1989).

⁷J. Teixeira, *On Growth and Form—Fractal and Non-fractal Patterns in Physics* (H. E. Stanley and N. Ostrovsky eds.), Martinus Nijhoff, Boston (1986), p. 145.

⁸H. D. Bale and P. W. Schmidt, Phys. Rev. Lett. **53**, 596 (1984).

⁹G. Lucido, R. Triolo, and E. Caponetti, Phys. Rev. B **38**, 9031 (1988).

¹⁰P.-Z. Wong, Phys. Rev. B **32**, 7417 (1985).

¹¹P.-Z. Wong, J. Howard, and J. S. Lin, Phys. Rev. Lett. **57**, 637 (1986).

¹²J. K. Kjems and P. Schofield, *Scaling Phenomena in Disordered Systems* (R. Pyne and A. Skjetorb eds.), Plenum, New York (1985) p. 133.

¹³L. Pietronero and E. Tosatti (eds.) *Fractals in Physics*, North-Holland, New York (1986).

¹⁴J. Rossat-Mignod, P. Bulet, M. J. Jurgens, C. Vettier, L. P. Regnault, J. Y. Henry, C. Ayache, L. Forro, H. Noel, M. Potel, P. Gougeon, and J. C. Levet, J. Phys. (Paris) **49** Coll. 8, 2119 (1988).

¹⁵L. A. Axelrod, G. P. Gordeev, I. M. Lazebnick, Mater. Sci. Forum **27/28**, 273 (1983).

¹⁶A. I. Okorokov, V. V. Runov, A. D. Tret'yakov *et al.*, Preprint No. 1526, Leningrad Inst. Nuclear Phys. (1989).

¹⁷V. E. Mikhailova, L. A. Aksel'rod, G. P. Gordeev *et al.*, Preprint No. 696, Leningrad Inst. Nuclear Phys. (1981).

¹⁸V. P. Khavronin, I. D. Luzyanin, and S. L. Ginzburg, Phys. Lett. A **129**, 399 (1988).

¹⁹S. G. Barsov, A. A. Vasil'ev, and A. L. Getalov *et al.*, Preprint No. 1438, Leningrad Inst. Nuclear Phys. (1988).

²⁰S. V. Maleev and B. P. Toperverg, Zh. Eksp. Teor. Fiz. **78**, 315 (1980) [Sov. Phys. JETP **51**, 158 (1980)].

Translated by R. Berman